Connecting the Water Phase Diagram to the Metastable Domain: High-Pressure Studies in the Supercooled Regime

ARTICLE *in* JOURNAL OF PHYSICAL CHEMISTRY LETTERS · NOVEMBER 2014

Impact Factor: 7.46 · DOI: 10.1021/jz501971h

7 AUTHORS, INCLUDING:

Margherita Citroni
University of Florence
38 PUBLICATIONS **427** CITATIONS
SEE PROFILE

Andrea Lapini
European Laboratory for Non-Linear Spectros…
23 PUBLICATIONS **115** CITATIONS
SEE PROFILE

Roberto Righini
University of Florence
171 PUBLICATIONS **4,049** CITATIONS
SEE PROFILE

THE JOURNAL OF PHYSICAL CHEMISTRY Letters

Letter

pubs.acs.org/JPCL

Connecting the Water Phase Diagram to the Metastable Domain: High-Pressure Studies in the Supercooled Regime

Samuele Fanetti,[†] Marco Pagliai,[‡] Margherita Citroni,[†,‡] Andrea Lapini,[†,‡] Sandro Scandolo,[§] Roberto Righini,[†,‡] and Roberto Bini*[,†,‡]

[†]LENS, European Laboratory for Nonlinear Spectroscopy, Via N. Carrara 1, I-50019 Sesto Fiorentino, Firenze, Italy

[‡]Dipartimento di Chimica "Ugo Schiff" dell'Università degli Studi di Firenze, Via della Lastruccia 3, I-50019 Sesto Fiorentino, Firenze, Italy

[§]The Abdus Salam International Centre for Theoretical Physics (ICTP), ICTP - Strada Costiera, 11, I-34151 Trieste, Italy

Supporting Information

ABSTRACT: Pressure is extremely efficient to tune intermolecular interactions, allowing the study of the mechanisms regulating, at the molecular level, the structure and dynamics of condensed phases. Among the simplest molecules, water represents in many respects a mystery despite its primary role in ruling most of the biological, physical, and chemical processes occurring in nature. Here we report a careful characterization of the dynamic regime change associated with low-density and high-density forms of liquid water by measuring the line shape of the OD stretching mode of HOD in liquid water along different isotherms as a function of pressure. Remarkably, the high-pressure studies have been here extended down to 240 K, well inside the supercooled regime. Supported by molecular dynamics simulations, a correlation among amorphous and crystalline solids and the two different liquid water forms is attempted to provide a unified picture of the metastable and thermodynamic regimes of water.

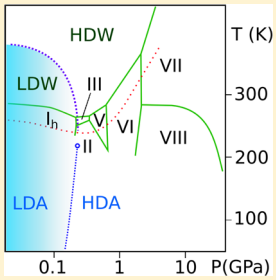

SECTION: Liquids; Chemical and Dynamical Processes in Solution

Water is the most abundant compound on the Earth surface, ruling life and being central to most of the chemical, biological, geological, and atmospheric processes. Despite that, the behavior of water in the condensed phases, peculiar under many respects, is not yet fully understood.[1] The main reason for the water distinctiveness is to be found in the presence of the hydrogen bonds, which rule the degree of molecular ordering in all of the phases and the peculiar pressure (P) and temperature (T) dependence of its physical properties.[2] In particular, the hydrogen bonds are extremely sensitive to the application of an external pressure, and this reflects in the role that water has in many processes taking place in the Earth's crust.[3]

Among the many anomalies exhibited by water that many theories and models have attempted to reconcile, particularly relevant is the existence of extended $P-T$ regions where water is in metastable forms, both as a supercooled liquid and as amorphous ice.[4−7] The connection between the local structures found in amorphous ices and those observed in the thermodynamic stable liquid phase is an issue of considerable interest animating the debate in the scientific community.[8−10] The understanding of this connection is made particularly challenging by the experimental difficulties that severely limit the laboratory studies in the supercooled regime where the water anomalies become more evident.[11] Among the models proposed to provide a comprehensive view of this complex scenario, two predict as counterparts of the two amorphous ices high-density and low-density liquids separated by a first-order transition or, possibly, coexisting and continuously transforming one into the other. In the first case, the phase transition implies the existence of a second critical point located in the "no man's land",[8] whose consequences extend into the supercooled and possibly within the $P-T$ range of thermodynamic stability of the liquid.[12] The "singularity-free" scenario instead predicts the existence of two liquid forms without implying any phase transition, as the two forms show a continuous reciprocal transformation[13,14] consisting of instantaneous modifications of the intermolecular organization.

Neutron diffraction studies provided evidence that on going from the low-density amorphous ice (LDA) to the high-density form (HDA) the molecules of the second coordination shell approach those of the first shell, entering in the interstitial volumes without any appreciable alteration of the size and structure of the first neighbor hydrogen-bonded tetrahedron.[15,16] These structural differences parallel those characterizing I_h ice and the high-pressure crystalline ices, the latter also presenting interpenetrating hydrogen-bond networks. This comparison is further extended to the thermodynamic stability region of the liquid where two local structures (LDW and HDW), remarkably differing in density, have been revealed by neutron diffraction studies.[17,18] Analysis of the O···O and O···H pair radial distribution functions ($g(r)$) showed that pressure

Received: September 17, 2014
Accepted: October 16, 2014
Published: October 16, 2014

   dx.doi.org/10.1021/jz501971h | J. Phys. Chem. Lett. 2014, 5, 3804−3809

drives the collapse of the second coordination shell onto the first one, which maintains its tetrahedral arrangement, a description also confirmed by classical molecular dynamics simulations.[19,20] The coexistence of two structurally different forms of water has been invoked to explain ambient pressure small-angle X-ray scattering[21] and optical Kerr effect experiments in the supercooled regime.[22] The relative amount of the two species changes with temperature, with the low-density form characterized by an LDA-type structure, being progressively favored upon cooling. Ultrafast transient infrared absorption spectra measured as a function of pressure and temperature further improved this view, highlighting the existence of two different dynamic regimes in the thermodynamic stability region of the liquid.[20] The rotational motion is accelerated by the insertion of second-shell molecules in the interstitial sites of the first shell because of the increased possible favorable tetrahedral configurations that can be realized. The completion of this insertion marks the attainment of the HDW regime. A similar mechanism was computationally predicted[23] and recently adopted to explain high-pressure quasi elastic neutron scattering results.[24] In the HDW regime, the rotational anisotropy decay is unaffected by the density increase, reflecting in a constant contribution to the line broadening and then to a less steep density dependence of the full width at half-maximum (fwhm) of the OD stretching band.[20] Quite remarkably, both experiments and computations (performed with ASAP[25] and SPC/E[26] force fields) agree that the slope change observed in the fwhm versus density plot nicely coincides with the density at which the time constant of the rotational anisotropy stops changing upon further compression.

In the attempt to connect the boundary between the two liquid forms to the metastable amorphous and crystalline ices domains, we performed a systematic investigation of the fwhm of the OD stretching mode as a function of pressure along different isothermal compression paths in the thermodynamic stability region of the liquid as well as in the supercooled regime. Infrared absorption spectra of solutions containing 3.5% D_2O in H_2O were measured by using a membrane anvil cell equipped with sapphires. The realization of the high-density configuration of the liquid, which marks the completed insertion of the second shell molecules onto the first one, was detected by the slope change of the fwhm of the OD stretching mode of the HOD molecule upon compression.[20] The OD stretching mode is indeed a good probe of the local structure,[27] and at the concentration employed, the OD oscillators are well-isolated so that the contribution to the line width of resonant energy transfer processes can be neglected.[28] Rotational and vibrational relaxation are responsible for the line broadening with increasing pressure or temperature. In particular, rotational relaxation has been identified as the major contribution to the broadening process of the OD stretching band in LDW, whereas its contribution does not change with pressure in HDW.[20]

We performed isothermal compression studies at 239.7, 247.3, 260.0, 318.0, and 339.0 K, which add to those at 273.7, 298.0, and 363.1 K already reported in ref 20. Remarkably, the two lowest compression experiments represent the first high-pressure optical experiments in the supercooled regime. In Figure 1, two representative set of spectra, at 239.7 and 363.1 K, are reported as a function of pressure. The fwhm of the OD stretching band, fit by a single Gaussian function, is reported for each isotherm as a function of the water density in Figure 2.

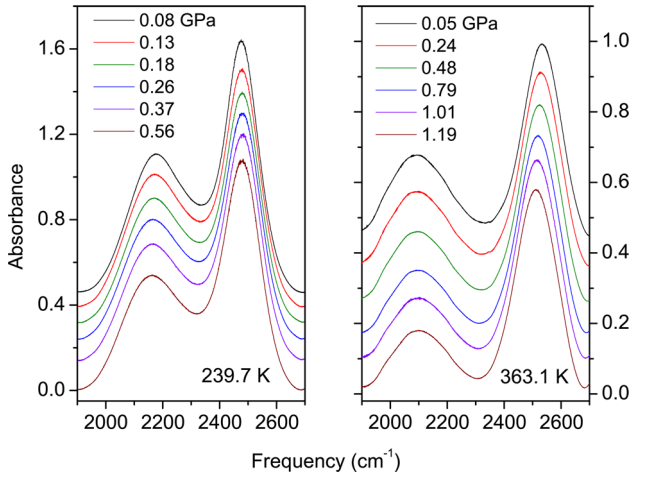

Figure 1. Evolution with pressure of the absorption spectra of a 3.5% solution of D_2O in H_2O in the OD stretching region at 239.7 (supercooled regime) and 363.1 K. The low-frequency band is due to the combination of bending and librational modes of H_2O (2175 cm^{-1} at 239.7 K and 0.08 GPa), whereas the high-frequency band is due to the OD stretching mode of HOD (2476 cm^{-1} at 239.7 K and 0.08 GPa).[29]

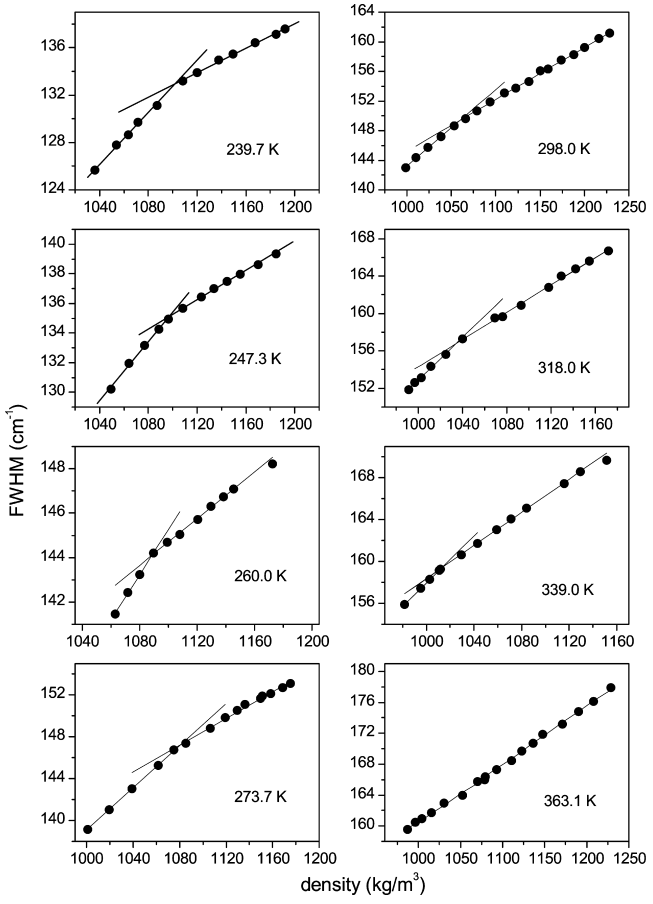

Figure 2. Evolution with density of the fwhm of the OD stretching band at different temperatures. The error bars relative to the density values determine the dot dimensions, whereas the error bars relative to the fwhm value are smaller. Two linear regimes have been identified at all temperatures, with the only exception of the data collected at 363.1 K.

dx.doi.org/10.1021/jz501971h | J. Phys. Chem. Lett. 2014, 5, 3804−3809

The density in the stability range of the liquid phase was computed according to the IAPWS-95,[30] whereas the density value for supercooled water was obtained from ref 31. For each isotherm, with the only exception of that at 363.1 K, the fwhm evolution with density was fit performing two linear regressions, one for the low-density and one for the high-density values. The intercept of the two lines corresponds to the point at which the dynamical regime becomes fully high density.[20] The slopes relative to the two regimes are shown in Figure 3. For

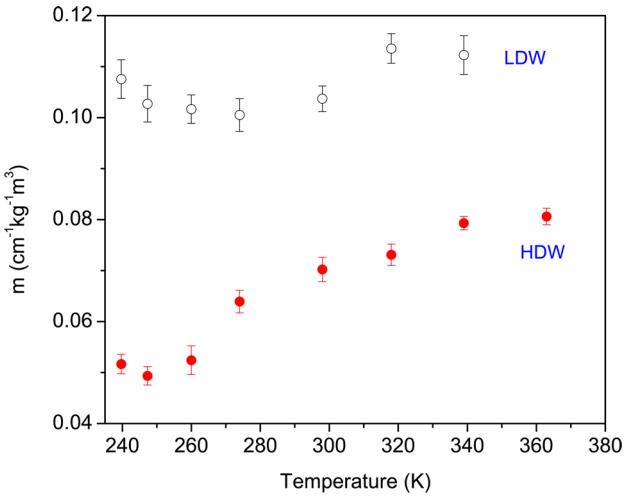

Figure 3. Temperature dependence of the slope (m) of the linear evolution employed to fit the fwhm versus density data in the low-density (empty dots) and high-density (full dots) regimes. Error bars refer to the linear regression analysis.

every temperature the slopes always remarkably reduce in the high-density regime because of the constant contribution of the rotational motion to the line broadening.[20] The data collected along the 363.1 K isotherm were fit by a straight line whose slope is characteristic of the HDW regime. (See Figure 3.)

Figure 4, upper panel, reports the density dependence of the OD peak frequency along different isothermal paths. Two pieces of evidence are worth commenting on. First, no changes in the density dependence of the peak frequency are observed, possibly related to the LDW and HDW regimes identified by the fwhm data. For temperatures higher than 273 K, the OD peak frequency monotonically softens with compression with a slope slightly increasing, as absolute value, with rising temperature. On the contrary, in the supercooled regime, the peak frequency first increases with density, reaching a maximum around 1110−1120 kg/m^3, and softens for further compression, as evidenced in the lower panel of Figure 4. The analysis of the dependence of the OH stretching frequency on density along isotherms has been used to speculate about a structural change regarding the hydrogen-bond network in liquid water.[32] Our results are consistent with the overall softening of the stretching frequencies due to the slight reduction of the O···O distance for increasing density. The anomalous increase in the frequencies at low densities in the supercooled regime could instead be compatible with a multicomponent picture of the stretching peak[33] in which a low-frequency component, manifestation of a low-density liquid local structure, dominates at low pressures and transfers intensity to a higher frequency mode for increasing density.

The phase diagram of water, comprehensive of all of the data points relative to the boundary between the two dynamic

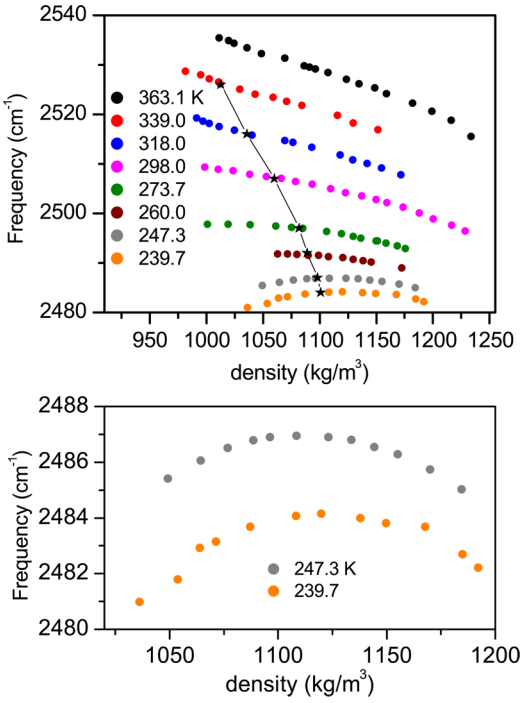

Figure 4. Upper panel: evolution with density of the peak frequency of the OD stretching band measured along the different isothermal compression paths; full stars indicate the density values at which the achievement of the high-density regime is completed as obtained by the slope change in the fwhm evolution with density. (See Figure 2.) Lower panel: detail of the density evolution of the OD stretching frequency measured at two different temperatures in the supercooled regime.

regimes identified by the slope change of the fwhm evolution with density of the OD stretching mode, is shown in Figure 5. Remarkably, the slope of this boundary becomes progressively smaller on lowering temperature and gets to coincide, within the experimental error, with the phase boundary between ices I and III. Farther extrapolation of this line in the supercooled regime and beyond reaches an area where several authors predicted the second critical point (CP2),[8,34−37] even though both higher[38] and lower[39,40] pressure values have been proposed for the CP2. Further extrapolation of this line by few tens of degrees in the "no man's land" brings to the crystallization line T_X, below which amorphous ices can form following different $P-T$ paths. (See, for example, ref 7.)

Many amorphous ices have been reported in the literature, and many other could likely be experimentally obtained. Among them, three main polyamorphic forms, namely, low-density (LDA), high-density (HDA), and very high-density (VHDA) amorphous ices, have been identified on the basis of the possible reversible mutual transitions and of general properties such as compressibility, pair radial distribution function, and number of interstitial molecules.[7] It should be remarked that the boundary separating LDA and HDA in Figure 5 is purely indicative because the transition between these ices is sensitive to the path followed.[7] The connection among these amorphous ice forms, the low- and high-density liquid forms, and the thermodynamically stable ice phases has been discussed by several authors. For example, the amorphous ices have been described as metastable frustrated structures of the underlying thermodynamically stable crystalline polymorphs due to the incomplete proton rearrangement.[41] The

dx.doi.org/10.1021/jz501971h | J. Phys. Chem. Lett. 2014, 5, 3804−3809

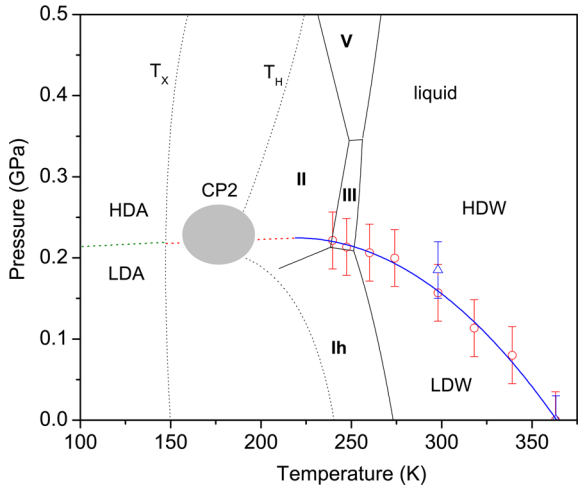

Figure 5. Relation between the phase diagram (boundaries identified by full lines) and the metastable forms of water (boundaries identified by dotted lines) below 0.5 GPa. The data points identifying the LDW and HDW liquid regimes are obtained by the slope changes in the fwhm versus density evolution as reported in Figure 2 (empty dots) and from the time domain rotational anisotropy measurements (empty triangles).[20] A cubic fit of these data is reported as a full blue line, above which only HDW exists. This line has been extrapolated in the "no man's land" (red dotted line) and connected to the hypothetical boundary separating LDA and HDA (green dotted line). The gray area represents the dispersion of the CP2 reported so far in literature.[8,34−37] The highest formation temperature (T_X) line of the amorphous ices and the homogeneous nucleation temperature (T_H) line, below which supercooling is not possible, are also reported (from ref 7).

possibility of exploring different metastable amorphous forms by changing the annealing pathway suggested kinetically controlled transformations, in particular, the formation of LDA, was ascribed to the incomplete transformation to crystalline ice, specifically to the I_h structure. As a matter of fact, a close resemblance between the structures of LDA and ice I_h was also pointed out on the basis of the similarities between the vibrational densities of states measured by incoherent neutron scattering[42] and between the X-ray Raman spectra in the postedge region.[43] The analogies between amorphous ices and liquid water were first remarked on by Finney et al.[16] through the analysis of $g(r)$, which represents the most consolidated approach to this purpose. A wealth of such experimental and computational data is available, and very similar modifications of the $g(r)$ have been observed on going from LDW (LDA) to HDW (HDA).[7,10,20] As a matter of fact, the high-density amorphous ices form through the contraction of the second-neighbor shell and the consequent increase in the local coordination. The additional molecules, belonging to the second shell in LDA, enter the interstitial sites: one molecule for HDA[16] and two molecules for VHDA.[44] However, these differences have also been related to the sample treatment because in situ neutron diffraction studies show that HDA and VHDA are very similar, at least up to the second shell.[45] This behavior parallels the one revealed by computations and experiments on liquid water, consisting of the collapse of the second-neighbor shell molecules onto the first one with rising pressure.[17−20] A comparison of computed $g(r)_{O\cdots O}$ of supercooled low-, high-, and very high-density water with those of ice phases I, III, and VI, respectively, shows close similarities.[46] In addition, it is worth remembering that the structural analogies between amorphous ices and the possible crystalline counterparts are not limited to the $g(r)$: also, the density of LDA is almost the same as ice I, and that of HDA almost coincides with those of ice II and ice III.[7,47] However, the comparison of different computational results should be made with caution because of the different potentials employed. Therefore, we performed molecular dynamics simulations under different thermodynamic conditions in both liquid- and solid-state with the ASAP force field,[25] which is particularly effective in the description of the structural and dynamic properties of liquid water in a broad range of pressure or temperature.[20] The $g(r)_{O\cdots O}$ represents a useful tool to describe the local environment and the different interactions that can be related to spectroscopic findings. Figure 6 collects the $g(r)_{O\cdots O}$

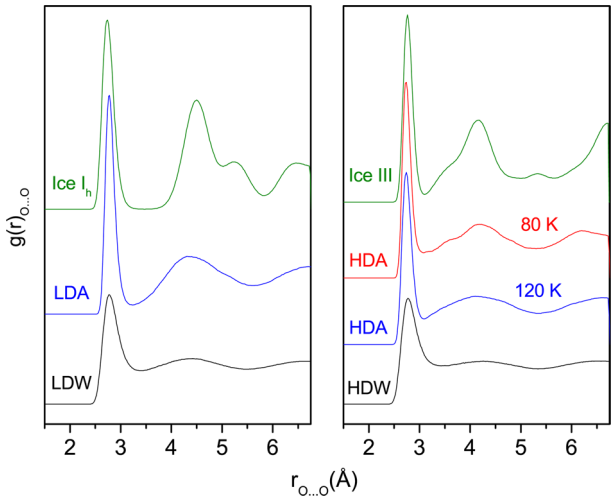

Figure 6. Pair radial distribution functions computed with the ASAP force field.[25] On the left panel, $g(r)$ of low-density liquid water (LDW) and amorphous ice (LDA) are compared with the I_h crystal; on the right panel, this comparison is performed among high-density liquid water (HDW) and amorphous ice (HDA), at two different temperatures, and the crystalline phase III.

computed for the ice and liquid forms of interest to the present discussion. Despite the remarkable broadening of the peaks on going from the crystal to the amorphous ice and then to the liquid, we can immediately appreciate the similarities of the position of the second maximum, related to the second shell molecules, in ice I, LDA, and LDW. The most remarkable difference passing from LDW to HDW is the filling of the minimum just above 3 Å that corresponds to the collapse of the second shell molecules onto the first one, as described in ref 20. The resemblance between HDW and HDA is explicit, especially when high-temperature HDA is considered. The effect of temperature, as also shown in ref 41, is in fact that of transferring population from the third (>4 Å) to the second (~3.5 Å) peak, making the $g(r)_{O\cdots O}$ of low-temperature HDA more similar to ice III.

Our experimental and computational data substantiate the correlation between metastable and thermodynamic phase diagram of water. The LDA and HDA ices can be considered the metastable counterparts of the underlying crystal phases I and III or II, respectively, and LDW and HDW, the two corresponding liquid water forms. The transformations among the different polyamorphs as well as between the crystalline and amorphous phases,[41,48] appear to be kinetically controlled. Remarkably, at temperatures below 250 K, the line dividing the metastable and thermodynamically stable high-density forms

dx.doi.org/10.1021/jz501971h | J. Phys. Chem. Lett. 2014, 5, 3804−3809

from the low-density ones almost coincides with a pressure value around 0.2 GPa. In fact, below 250 K, pressure appears as the only factor effective in modifying the intermolecular interaction geometry. In a simplified approach we can imagine a potential energy landscape reflecting the complexity of the hydrogen-bonded network. Below 250 K and 0.2 GPa the low-density crystalline and amorphous solids are the most stable forms, and they are likely characterized by energy barriers that cannot be thermally overcome. Conversely, the variation of pressure is extremely efficient in changing the profile of the potential energy landscape through the modification of the nearest neighbor arrangement of water molecules, thus leading to the realization of high-density configurations. Above 250 K, as the melting occurs, temperature becomes more and more effective and favors, also at constant pressure, a progressively easier interpenetration of the second shell.

The interpretation of the present data does not require the presence of a CP2 in the "no man's land", as the regime change between LDW and HDW is continuous and associated with a variation of the local dynamics driven by the collapse of the second shell molecules. LDW and HDW are the liquid counterparts of LDA and HDA, which in turn are the metastable forms of low- and high-density crystalline ices I and III (or II), respectively. The phase diagram of condensed water can be therefore divided in two macroscopic regions characterized by strong local structural similarities, each one containing fluid, amorphous, and crystalline phases. Remarkably, above 0.25 GPa and 363 K, only the high-density forms exist.

METHODS

A detailed description of the experimental and computational methods is reported in the Supporting Information.

ASSOCIATED CONTENT

Supporting Information

Detailed description of the experimental and computational methods. This material is available free of charge via the Internet at http://pubs.acs.org.

AUTHOR INFORMATION

Corresponding Author

*E-mail: roberto.bini@unifi.it.

Notes

The authors declare no competing financial interest.

ACKNOWLEDGMENTS

Supported by Deep Carbon Observatory initiative under the project *Physics and Chemistry of Carbon at Extreme Conditions* (grant from the Alfred P. Sloan Foundation) and by MIUR (grant FIRB - Futuro in Ricerca 2010 RBFR109ZHQ).

REFERENCES

(1) Ball, P. Water - an Enduring Mystery. *Nature* **2008**, *452*, 291–292.

(2) *Water, a Comprehensive Treatise*; Franks, F., Ed.; Plenum Press: New York, 1972–1982.

(3) Geophysics Study Committee; et al. *The Role of Fluids in Crustal Processes*; National Academies Press: Washington, DC, 1990.

(4) Mishima, O.; Calvert, L. D.; Whalley, E. 'Melting Ice' I at 77 K and 10 kbar: a New Method of Making Amorphous Solids. *Nature* **1984**, *310*, 393–395.

(5) Mishima, O.; Calvert, L. D.; Whalley, E. An Apparently 1st-Order Transition Between Two Amorphous Phases of Ice Induced by Pressure. *Nature* **1985**, *314*, 76–78.

(6) Mishima, O. Reversible First-Order Transition Between Two H_2O Amorphs at ~0.2 GPa and ~135 K. *J. Chem. Phys.* **1994**, *100*, 5910–5912.

(7) Loerting, T.; Winkel, K.; Seidl, M.; Bauer, M.; Mitterdofer, C.; Handle, P. H.; Salzmann, C. G.; Mayer, E.; Finney, J. L.; Bowron, D. T. How Many Amorphous Ices are There? *Phys. Chem. Chem. Phys.* **2011**, *13*, 8783–8794.

(8) Poole, P. H.; Sciortino, F.; Essmann, U.; Stanley, H. E. Phase Behaviour of Metastable Water. *Nature* **1992**, *360*, 324–328.

(9) Mishima, O.; Stanley, H. E. The Relationship Between Liquid, Supercooled and Glassy Water. *Nature* **1998**, *396*, 329–335.

(10) Soper, A. K. Structural Transformations in Amorphous Ice and Supercooled Water and Their Relevance to the Phase Diagram of Water. *Mol. Phys.* **2008**, *106*, 2053–2076.

(11) Debenedetti, P. G. Supercooled and Glassy Water. *J. Phys. Condens. Matter* **2003**, *15*, R1669–R1726.

(12) Xu, L. M.; Kumar, P.; Buldyrev, S. V.; Chen, S. H.; Poole, P. H.; Sciortino, F.; Stanley, H. E. Relation Between the Widom Line and the Dynamic Crossover in Systems with a Liquid-Liquid Phase Transition. *Proc. Natl. Acad. Sci. U.S.A.* **2005**, *102*, 16558–16562.

(13) Sastry, S.; Debenedetti, P. G.; Sciortino, F.; Stanley, H. E. Singularity-Free Interpretation of the Thermodynamics of Supercooled Water. *Phys. Rev. E* **1996**, *53*, 6144–6154.

(14) Rebelo, L. P. N.; Debenedetti, P. G.; Sastry, S. Singularity-Free Interpretation of the Thermodynamics of Supercooled Water. II. Thermal and Volumetric Behavior. *J. Chem. Phys.* **1998**, *109*, 626–633.

(15) Klotz, S.; Hamel, G.; Loveday, J. S.; Nelmes, R. J.; Guthrie, M.; Soper, A. K. Structure of High-Density Amorphous Ice under Pressure. *Phys. Rev. Lett.* **2002**, *89*, 285502.

(16) Finney, J. L.; Hallbrucker, A.; Kohl, I.; Soper, A. K.; Bowron, D. T. Structures of High and Low Density Amorphous Ice by Neutron Diffraction. *Phys. Rev. Lett.* **2002**, *88*, 225503.

(17) Soper, A. K.; Ricci, M. A. Structures of High-Density and Low-Density Water. *Phys. Rev. Lett.* **2000**, *84*, 2881–2884.

(18) Strässle, Th.; Saitta, A. M.; Le Godec, Y.; Hamel, G.; Klotz, S.; Loveday, J. S.; Nelmes, R. J. Structure of Dense Liquid Water by Neutron Scattering to 6.5 GPa and 670 K. *Phys. Rev. Lett.* **2006**, *96*, 067801.

(19) Saitta, A. M.; Datchi, F. Structure and Phase Diagram of High-Density Water: The Role of Interstitial Molecules. *Phys. Rev. E* **2003**, *67*, 020201.

(20) Fanetti, S.; Lapini, A.; Pagliai, M.; Citroni, M.; Di Donato, M.; Scandolo, S.; Righini, R.; Bini, R. Structure and Dynamics of Low-Density and High-Density Liquid Water at High Pressure. *J. Phys. Chem. Lett.* **2014**, *5*, 235–240.

(21) Huang, C.; Wikfeldt, K. T.; Tokushima, T.; Nordlund, D.; Harada, Y.; Bergmann, U.; Niebuhr, M.; Weiss, T. M.; Horikawa, Y.; Leetmaa, M.; et al. The Inhomogeneous Structure of Water at Ambient Conditions. *Proc. Natl. Acad. Sci. U.S.A.* **2009**, *106*, 15214–15218.

(22) Taschin, A.; Bartolini, P.; Eramo, R.; Righini, R.; Torre, R. Evidence of Two Distinct Local Structures of Water from Ambient to Supercooled Conditions. *Nat. Commun.* **2013**, *4*, 2401.

(23) Laage, D.; Hynes, J. T. A Molecular Jump Mechanism of Water Reorientation. *Science* **2006**, *311*, 832–835.

(24) Bove, L. E.; Klotz, S.; Strässle, Th.; Koza, M.; Teixeira, J.; Saitta, A. M. Translational and Rotational Diffusion in Water in the Gigapascal Range. *Phys. Rev. Lett.* **2013**, *111*, 185901.

(25) Pinilla, C.; Irani, A. H.; Seriani, N.; Scandolo, S. Ab Initio Parameterization of an All-Atom Polarizable and Dissociable Force Field for Water. *J. Chem. Phys.* **2012**, *136*, 114511.

(26) Berendsen, H. J. C.; Grigera, J. R.; Straatsma, T. P. The Missing Term in Effective Pair Potentials. *J. Phys. Chem.* **1987**, *91*, 6269–6271.

(27) Moilanen, D. E.; Fenn, E. E.; Lin, Y.-S.; Skinner, J. L.; Bagchi, B.; Fayer, M. D. Water Inertial Reorientation: Hydrogen Bond Strength

and the Angular Potential. *Proc. Natl. Acad. Sci. U.S.A.* **2008**, *105*, 5295−5300.
(28) Piatkowski, L.; Eisenthal, K. B.; Bakker, H. J. Ultrafast Intermolecular Energy Transfer in Heavy Water. *Phys. Chem. Chem. Phys.* **2009**, *11*, 9033−9038.
(29) Walrafen, G. E. Raman and Infrared Spectral Investigations of Water Structure. In *Water: A Comprehensive Treatise*; Franks, F, Ed.; Plenum Press, New York, 1972; pp 151−214.
(30) Wagner, W.; Pruss, A. The IAPWS Formulation 1995 for the Thermodynamic Properties of Ordinary Water Substance for General and Scientific Use. *J. Phys. Chem. Ref. Data* **2002**, *31*, 387−535.
(31) Mishima, O. Volume of Supercooled Water Under Pressure and the Liquid-Liquid Critical Point. *J. Chem. Phys.* **2010**, *133*, 144503.
(32) Kawamoto, T.; Ochiai, S.; Kagi, H. Changes in the Structure of Water Deduced from the Pressure Dependence of the Raman OH Frequency. *J. Chem. Phys.* **2004**, *120*, 5867−5870.
(33) Mallamace, F.; Broccio, M.; Corsaro, C.; Faraone, A.; Majolino, D.; Venuti, V.; Liu, L.; Mou, C.-Y.; Chen, S.-H. Evidence of the Existence of the Low-Density Liquid Phase in Supercooled, Confined Water. *Proc. Natl. Acad. Sci. U.S.A.* **2007**, *104*, 424−428.
(34) Poole, P. H.; Essmann, U.; Sciortino, F.; Stanley, H. E. Phase Diagram for Amorphous Solid Water. *Phys. Rev. E* **1993**, *48*, 4605−4610.
(35) Kiselev, S. B.; Ely, J. F. Parametric Crossover Model and Physical Limit of Stability in Supercooled Water. *J. Chem. Phys.* **2002**, *116*, 5657−5665.
(36) Dougherty, R. C. The PVT Surface of Water: Critical Phenomena Near 0.195 GPa, 182 K. *Chem. Phys.* **2004**, *298*, 307−315.
(37) Kanno, H.; Miyata, K. The Location of the Second Critical Point of Water. *Chem. Phys. Lett.* **2006**, *422*, 507−512.
(38) Stanley, H. E.; Barbosa, M. C.; Mossa, S.; Netz, P. A.; Sciortino, F.; Starr, F. W.; Yamada, M. Statistical Physics and Liquid Water at Negative Pressures. *Physica A* **2002**, *315*, 281−289.
(39) Jeffery, C. A.; Austin, P. H. A New Analytic Equation of State for Liquid Water. *J. Chem. Phys.* **1999**, *110*, 484−496.
(40) Mishima, O. Volume of Supercooled Water Under Pressure and the Liquid-Liquid Critical Point. *J. Chem. Phys.* **2010**, *133*, 144503.
(41) Tse, J. S.; Klug, D. D. Pressure Amorphized Ices - an Atomistic Perspective. *Phys. Chem. Chem. Phys.* **2012**, *14*, 8255−8263.
(42) Klug, D. D.; Tulk, C. A.; Svensson, E. C.; Loong, C. K. Dynamics and Structural Details of Amorphous Phases of Ice Determined by Incoherent Inelastic Neutron Scattering. *Phys. Rev. Lett.* **1999**, *83*, 2584−2587.
(43) Tse, J. S.; Shaw, D. M.; Klug, D. D.; Patchkovskii, S.; Vankó, G.; Monaco, G.; Krisch, M. X-ray Raman Spectroscopic Study of Water in the Condensed Phases. *Phys. Rev. Lett.* **2008**, *100*, 095502.
(44) Finney, J. L.; Bowron, D. T.; Soper, A. K.; Loerting, T.; Mayer, E.; Hallbrucker, A. Structure of a New Dense Amorphous Ice. *Phys. Rev. Lett.* **2002**, *89*, 205503.
(45) Klotz, S.; Strässle, T.; Saitta, A. M.; Rousse, G.; Hamel, G.; Nelmes, R. J.; Loveday, J. S.; Guthrie, M. In Situ Neutron Diffraction Studies of High Density Amorphous Ice Under Pressure. *J. Phys.: Condens. Matter* **2005**, *17*, S967−S974.
(46) Jedlovsky, P.; Pártay, L. B.; Bartók, A. P.; Garberoglio, G.; Vallauri, R. Structure of Coexisting Liquid Phases of Supercooled Water: Analogy with Ice Polymorphs. *J. Chem. Phys.* **2007**, *126*, 241103.
(47) Loerting, T.; Bauer, M.; Kohl, I.; Watschinger, K.; Winkel, K.; Mayer, E. Cryoflotation: Densities of Amorphous and Crystalline Ices. *J. Phys. Chem. B* **2011**, *115*, 14167−14175.
(48) Chen, J. Y.; Yoo, C. S. High Density Amorphous Ice at Room Temperature. *Proc. Natl. Acad. Sci. U.S.A.* **2011**, *108*, 7685−7688.